

Hysteresis in superconducting short weak links and μ -SQUIDS

Dibyendu Hazra¹, Lætitia Pascal², Hervé Courtois², and Anjan K. Gupta¹

¹*Department of Physics, Indian Institute of Technology Kanpur, Kanpur 208016, India and*

²*Institut Néel, CNRS and Université Joseph Fourier, 25 avenue des Martyrs, Grenoble, France.*

(Dated: September 28, 2018)

Thermal hysteresis in a micron-size Superconducting Quantum Interference Device (μ -SQUID), with weak links as Josephson junctions, is an obstacle for improving its performance for magnetometry. Following the “hot-spot” model of Skocpol et al. [J. Appl. Phys. **45**, 4054 (1974)] and by incorporating the temperature dependence of thermal conductivity of superconductor using a linear approximation, we find a much better agreement with the observed temperature dependence of the retrapping current in short superconducting Nb-based weak links and μ -SQUIDS. In addition, using the temperature dependence of the critical current, we find that above a certain temperature hysteresis disappears. We analyze the current-voltage characteristics and the weak link temperature variation in both the hysteretic and non-hysteretic regimes. We also discuss the effect of the weak link geometry in order to widen the temperature range of hysteresis-free operation.

I. INTRODUCTION

A micron-size superconducting quantum interference device (μ -SQUID) consists of two superconducting Dayem bridges or weak links (WL) [1], of dimension of the order of the superconducting coherence length, in parallel, forming a loop with area in the μm^2 range. A single WL behaves very much like a Josephson Junction [1] with the supercurrent approximately given by $I = I_c \sin\theta$, where I_c is the critical current and θ is the phase difference across the junction. When two such junctions are fabricated in parallel in a SQUID, interference between the two current branches gives an oscillatory behavior of the critical current I_c with the external magnetic field [2]. The flux period is equal to the flux quanta $\Phi_0 = 2.05 \times 10^{-15} \text{ T.m}^2$. This makes the SQUID a very sensitive device to measure magnetic field. While the flux sensitivity achieved by conventional SQUIDS is better than $10^{-7} \Phi_0 / \sqrt{Hz}$, for a μ -SQUID it has only been about $10^{-4} \Phi_0 / \sqrt{Hz}$ [3]. μ -SQUIDS have been used to study the magnetization reversal [3] of an isolated magnetic nano particle, the persistent current in phase-coherent rings [4] and also in scanning SQUID microscopy [5]. An improved sensitivity of μ -SQUIDS would be useful for probing ferromagnetic particles of smaller size or where the surface spins play an important role [6].

Other than the sensitivity, the hysteresis in μ -SQUIDS current-voltage (I-V) characteristic (see e.g. Ref. 5) is a major hurdle as it (1) increases the measurement time, (2) complicates the measurement electronics, (3) changes the temperature of the sample placed in close proximity with the μ -SQUID. Thus it is important to understand this hysteresis and devise ways of eliminating it. Hysteresis in the current-voltage characteristic is a very common phenomena for many superconducting nano-structured systems, especially WLs. It includes conventional Superconductor-Insulator-Superconductor (S-I-S) Josephson junctions [2], Superconductor-Normal metal-Superconductor (S-N-S) junctions [7, 8], superconducting nano-wires [9] and superconducting μ -bridges [10–12].

When the current is ramped up from zero across such junctions, the system suddenly switches to a non-zero voltage state at the critical current I_c . After switching, when the current is ramped down, the system comes back to a zero-voltage state at a particular current, called the retrapping current I_r . At very low temperature, the retrapping current can be smaller than the critical current: $I_r < I_c$. This defines an hysteretic I-V curve.

A number of models have been proposed in the last few decades to understand the hysteresis in superconducting WLs. The resistively and capacitively shunted junction (RCSJ) [2] model predicts the I-V curve for a conventional S-I-S junction very well. In this case, the capacitance across the junction is responsible for the hysteresis. But for lateral junctions (either S-N-S junctions or constrictions), the geometrical capacitance is too small to explain hysteresis. Hence an alternative theory of an effective capacitance C_{eff} was proposed [12], where one equates the charge relaxation time $R_n C_{eff}$ with the Cooper pair relaxation time \hbar/Δ . Here R_n is the normal resistance and Δ is the superconducting gap parameter. The same method was recently extended to S-N-S junctions [7] by equating $R_n C_{eff}$ with the diffusion time of Andreev pairs. Though these methods reproduce some of the features of the I-V curves, no justification behind the origin of an effective capacitance has been found.

Recently, Courtois et al. [13] have unambiguously shown, by directly measuring the electronic temperature, that heating is responsible for hysteresis in S-N-S junctions. According to the “hot-spot” model of Skocpol et al. [11], the heat generated in the resistive region of the WL raises locally its temperature above the critical temperature T_c . The temperature goes down to the bath temperature as one moves away from the hot spot. This gives rise to a normal metal-superconductor interface along the surface defined by $T = T_c$. The interface location is self-consistently determined by the heat generated and the coupling to the thermal bath. It was found that below a certain current, identified as the retrapping current, this interface becomes unsustainable and the WL turns fully superconducting. For a short WL, the hot

spot may spread beyond the WL and into the electrodes. This “hot-spot” model reproduced most of the features of the I-V characteristics of superconducting WLs. It also predicted a $\sqrt{1 - T/T_c}$ dependence of I_r on T ; however the latter was not experimentally verified. Further, this model ignored the temperature dependence of the thermal conductivity of superconductor. Incorporating an approximate form for this temperature dependence, Tinkham et al. described the I-V characteristics of free standing superconducting nano-wires [14]. In this case, the N-S interface occurs inside the long nano-wire, making the problem one-dimensional. Again, this work did not include the temperature dependence of the hysteresis in the I-V characteristics.

In this paper, we describe an effective one-dimensional thermal model to find out the temperature profile near a short WL connected to wide electrodes. We calculate the I-V characteristics as well as the (bath) temperature dependence of the retrapping current. Our model predicts how the normal-superconducting (N-S) interface position varies with various parameters like temperature, current, and geometry. We also discuss the detailed temperature profile and how it changes with the bias current. Using the temperature dependence of the critical current near T_c , we find that above a certain temperature T_h , hysteresis disappears. The effect of the WL geometrical parameters on T_h is discussed quantitatively. As the same model is directly relevant to μ -SQUIDs, we test it on several such samples. Our model fits our data very well. Finally, we discuss how the non-hysteretic regime can be achieved over a wider temperature range, followed by conclusions.

II. THERMAL MODEL OF HYSTERESIS

Following the “hot-spot” model [11], we consider a single WL connected to two extended electrodes, as shown in Fig. 1a, and investigate the temperature distribution around it in the resistive state. We assume a local quasi-equilibrium condition so that a local temperature can be defined at each point of the sample. The length and width of the WLs under study are in 50-200 nm range, i.e. of the order of the coherence length of bulk Nb ($\xi_{Nb} \approx 39$ nm). In this range, a WL behaves very much like a Josephson Junction [1]. Since the WL size is very small, we assume that in the resistive state the entire WL region stays at a uniform temperature. In reality, the WL will have certain spatial temperature variation, but what will matter here is the heat evacuated out of the WL. This assumption will not affect our conclusions as long as the WL temperature is not so large as to affect its resistance. We also assume the pads connecting to the WLs to be much wider than the length scale over which the temperature relaxes to the bath temperature.

At a given bias current, we can divide the device into three regions as shown in Fig. 1b: 1) the narrow WL at a uniform temperature T_1 consisting of the rectangular

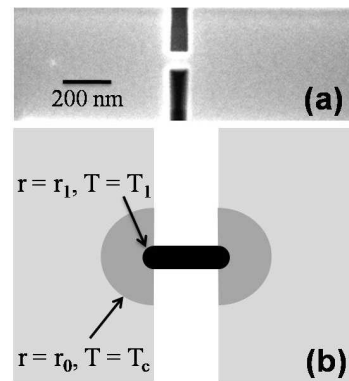


FIG. 1: (a) Scanning electron micrograph image of a WL. (b) Sketch of the sample geometry with the three regions discussed in the text.

(width w and length l) area in the center and terminating into a semicircle of radius $r_1 = w/2$ at each end, 2) a normal state ($T > T_c$) semicircular region in each electrode with $r_0 > r > w/2$, and 3) a superconducting ($T < T_c$) region for $r > r_0$. We have assumed a rounded WL of radius $r_1 = w/2$ to avoid logarithmic divergence in the resistance calculation. This approach is unlike the hot spot model for a long WL [11], where the hot-spot develops near the center of the WL. Beyond the WL, we assume that the heat conducts away radially in the bulk of the film. Thus the temperature also decreases radially inside the two electrodes, reaching the bath temperature T_b far away from the WL. This enables us to use an effective one-dimensional model for finding the spatial variation of temperature. The source of heat is the resistive dissipation in the normal region, which extends up to a radial distance r_0 in each electrode, thus defining a N-S interface with $T = T_c$ between normal and superconducting regions.

In the resistive state, the Joule heat near the WL region is removed in two ways: conduction within each electrode and surface heat flow from film’s bottom surface to the substrate. The latter is assumed to be proportional to the temperature difference between the film and the substrate. This approximation has been used extensively [11, 15, 16]; we will discuss its validity later. We neglect the heat loss from the top surface of the film as we operate in a vacuum cryostat. We also assume that the entire substrate stays at the bath temperature T_b . Thus, the general heat flow equation can be written as:

$$-\kappa \frac{dT}{dr} 2\pi r d + \int_{r_1}^r \alpha (T - T_b) 2\pi r dr + \alpha (T_1 - T_b) A = I^2 R(r). \quad (1)$$

Here κ is the thermal conductivity, d is the thickness of the film, A is the area of the WL region given by $A = (wl + \pi r_1^2)$, I is the current. The surface heat loss coefficient α is expressed in W/m^2K . $R(r)$ is the resistance of the electrode within a radius r including the resistance of the WL. Assuming a radial and isotropic cur-

rent flow in the electrodes giving rise to circular equipotential lines, the resistance $R(r)$ is given by:

$$R(r) = R_0 + R_c \ln\left(\frac{r}{r_1}\right), \quad (2)$$

where $\pi R_c/2 = \rho_N/d$ is the square resistance of the film, with ρ_N as the normal state resistivity. Thus R_c defines a characteristic resistance of the film. The resistance R_0 of the WL is given by $R_0 = (l + 2r_1)\rho_N/wd$.

Since we consider low temperatures, we ignore the phonon's contribution to the thermal conductivity. In the normal state, the electronic part of the thermal conductivity κ_n can be found using the Wiedemann-Franz law: $\kappa_n = L_0 T/\rho_N$, where κ_n is the thermal conductivity in the normal state and L_0 is the Lorentz number. In the superconducting state, as the number of quasi-particles decreases significantly, one expects the thermal conductivity κ_s to be much less. At very low temperature, since only very few quasi-particles are left to carry thermal energy, κ_s can be exponentially small. We use here a linear approximation, $\kappa_s/\kappa_n = T/T_c$, which gives $\kappa_s = \kappa_n$ at $T = T_c$ as expected. From the theory [17], this linear approximation is well justified near T_c . The same approximation was also used by Tinkham et al. [14].

Using the above expressions for κ and $R(r)$ and differentiating Eq. 1 with respect to r , one gets:

$$\frac{1}{r} \frac{d}{dr} \left[rT \frac{dT}{dr} \right] - \frac{\rho_N \alpha}{L_0 d} (T - T_b) = - \left(\frac{I \rho_n}{\pi d} \right)^2 \frac{1}{L_0 r^2}, \quad (r_1 \leq r < r_0) \quad (3)$$

$$\frac{1}{r} \frac{d}{dr} \left[rT^2 \frac{dT}{dr} \right] - \frac{\rho_N \alpha T_c}{L_0 d} (T - T_b) = 0 \quad (r > r_0). \quad (4)$$

The boundary conditions are: 1) at $r = r_1$, $T = T_1$ and Eq. 1 gives $-\kappa(T_1) \frac{dT}{dr} 2\pi r_1 d + \alpha(T_1 - T_b)A = I^2 R_0$, 2) at $r = r_0$, $T = T_c$, T and $\frac{dT}{dr}$ are continuous and 3) for $r \rightarrow \infty$, $T = T_b$. The radius r_0 and WL temperature T_1 have to be found self-consistently using these boundary conditions.

An inspection of the above two equations gives us a length scale,

$$\eta = \sqrt{\frac{L_0 T_c d}{\alpha \rho_N}} = \sqrt{\frac{2L_0 T_c}{\pi \alpha R_c}} \quad (5)$$

and a current scale

$$I_0 = \frac{\pi d T_c}{\rho_N} \sqrt{L_0} = \frac{2T_c}{R_c} \sqrt{L_0} = \frac{\pi \alpha}{\sqrt{L_0}} \eta^2. \quad (6)$$

Here I_0 would determine the scale of the retrapping current I_r , while η would determine the length scale of temperature variation. For WLs based on a Nb film deposited on a Si substrate, one typically uses a thickness of 20 to 150 nm. Depending upon the detailed preparation method, some typical parameters would be $\rho_N = 15\text{-}50 \mu\Omega \text{ cm}$, $T_c = 6\text{-}9 \text{ K}$ and $\alpha = 1\text{-}3 \text{ W/cm}^2 \text{ K}$ [15].

Using $L_0 = 2.44 \times 10^{-8} \text{ W}\cdot\Omega/\text{K}^2$, we get $\eta \sim 1\text{-}3 \mu\text{m}$ and $I_0 \sim 0.5\text{-}2 \text{ mA}$.

Eq. 3 and 4 can be written in terms of the dimensionless variables $x = r/\eta$, $t = T/T_c$, $i = I/I_0$, $x_1 = r_1/\eta$, $x_0 = r_0/\eta$ and $t_b = T_b/T_c$ as follows:

$$\frac{1}{x} \frac{d}{dx} \left[xt \frac{dt}{dx} \right] - (t - t_b) = -\frac{i^2}{x^2} \quad (x_1 \leq x < x_0), \quad (7)$$

$$\frac{1}{x} \frac{d}{dx} \left[xt^2 \frac{dt}{dx} \right] - (t - t_b) = 0 \quad (x > x_0). \quad (8)$$

In terms of the reduced variables, the boundary conditions become: 1) at $x = x_1$, $-x_1 t_1 \frac{dt}{dx} + (t_1 - t_b) \frac{A}{2\pi\eta^2} = \frac{\pi d R_0}{2\rho_N} i^2$, 2) at $x = x_0$, $t = 1$ and dt/dx is continuous, and 3) for $x \rightarrow \infty$, $t = t_b$. For short weak links, using $\frac{A}{2\pi\eta^2} \ll 1$, the first boundary condition becomes $t_1 \frac{dt}{dx} = -\beta i^2/x_1$ with $\beta = \frac{\pi R_0 d}{2\rho_N} = \frac{R_0}{R_c} \cong \frac{\pi}{2} (1 + \frac{\ell}{w})$.

Eq. 7 and 8 are second order and non-linear differential equations that can be solved only numerically. We wish to go beyond the approximation of κ being independent of temperature, which would give solutions in terms of modified Bessel functions as discussed by Skocpol et al.[11]. We choose to simplify the above equations by substituting $y_1 = t^2$ and $y_2 = t^3$ in Eq. 7 and 8, respectively. y_1 and y_2 then satisfy:

$$\frac{d}{dx} \left[x \frac{dy_1}{dx} \right] = -\frac{2i^2}{x} + 2(\sqrt{y_1} - t_b)x \quad (x_1 \leq x < x_0), \quad (9)$$

$$\frac{d}{dx} \left[x \frac{dy_2}{dx} \right] = 3(y_2^{1/3} - t_b)x \quad (x > x_0) \quad (10)$$

Let us first consider the superconducting region ($x > x_0$) described by Eq. 10. In this equation, y_2 varies between t_b^3 and 1. For this range of y_2 , we linearly approximate the $(y_2^{1/3} - t_b)$ term as:

$$y_2^{1/3} - t_b \approx \frac{y_2 - t_b^3}{1 + t_b + t_b^2}, \quad (11)$$

so as to keep the end points of $(y_2^{1/3} - t_b)$, i.e. 0 at $t = t_b$ and $(1 - t_b)$ at $t = 1$, fixed. This approximation becomes more and more accurate as t_b approaches 1, i.e. the bath temperature T_b approaches the critical temperature T_c . Eq. 10 then reduces to the modified Bessel equation $s^2 \xi'' + s \xi' - s^2 \xi = 0$, where $\xi = y_2 - t_b^3$ and $s = \lambda x$ with $\lambda = \sqrt{3/(1 + t_b + t_b^2)}$. With the boundary condition $t = t_b$ (i.e. $\xi = 0$) at $x \rightarrow \infty$, the only acceptable solution is $\xi = CK_0(s)$, where K_0 is the modified Bessel function of second kind and zero degree. Using the boundary condition $t = 1$ at $x = x_0$, we get the final solution for $x > x_0$ as:

$$t^3 = t_b^3 + \frac{1 - t_b^3}{K_0(\lambda x_0)} K_0(\lambda x). \quad (12)$$

Fig. 2 shows for comparison the numerical solution of the non-linear Eq. 10 and the corresponding solution to

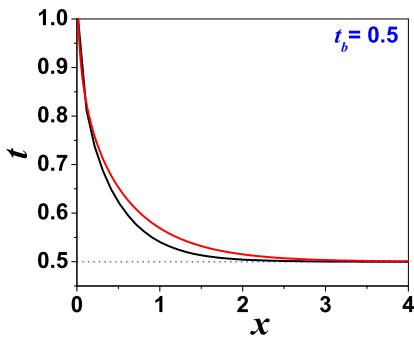


FIG. 2: Comparison between exact (Eq. 11, black) and approximate (Eq. 12, red) solution for the reduced temperature profile for $x > x_0$. The respective calculated slopes at the origin are - 5.1 and - 4.80. Parameters are $t_b = 0.5$ and $x_0 = 0.015$.

the linearized Eq. 12 for $t_b = 0.5$ and $x_0 = 0.015$. The overall shapes of the curves are similar, justifying our approximation.

Let us now consider the normal region ($x < x_0$). Eq. 9 is difficult to linearize as y_1 varies between t_b and t_1 , and t_1 is not known before-hand. The nature of boundary conditions does not allow a simple numerical solution. We make the approximation to neglect the surface loss term, i.e. the $(\sqrt{y_1} - t_b)$ term in Eq. 9. This is justified for finding the retrapping current I_r in the regime $x_0 \gtrsim x_1$, in which case the heat loss to the substrate is not significant as compared to the heat conducted out. With this approximation, there is an analytical solution: $y_1 = -i^2 [(\ln x + C_1)^2 + C_2]$. Here C_1 and C_2 are constants to be found from the boundary conditions: $y_1 = t^2 = 1$ at $x = x_0$ and $dy_2/dx = -2\beta i^2/x_1$. Finally, we get for $x_1 < x < x_0$:

$$t^2 = 1 - i^2 \left[\left(\ln \frac{x}{x_1} + \beta \right)^2 - \left(\ln \frac{x_0}{x_1} + \beta \right)^2 \right]. \quad (13)$$

This relation gives the temperature profile for $x < x_0$ and determines the WL temperature $t_1 = t(x_1)$ in terms of x_0 . To find x_0 , we have to use the continuity of dt/dx at x_0 using solutions given by Eq. 12 and 13. This gives the following transcendental equation for x_0 :

$$i^2 = \frac{\lambda x_0 (1 - t_b^3) K_1(\lambda x_0)}{3 [\ln(x_0/x_1) + \beta] K_0(\lambda x_0)}. \quad (14)$$

As shown in Fig. 3a, the right hand side of above Eq. 14 features a minima in current i as a function of x_0 . This means that below this current, the Joule heat is not sufficient to uphold a normal metal-superconductor (N-S) interface with $T = T_c$. This current is thus identified as the retrapping current $i_r = I_r/I_0$. Fig. 3b shows that it decreases with increasing bath temperature, whereas the related x_0 increases. At high temperature, a regime where the retrapping current exceeds the critical current ($i_r > i_c$) can be reached. In this case, the WL is resistive while its temperature stays below T_c . Only if the bias

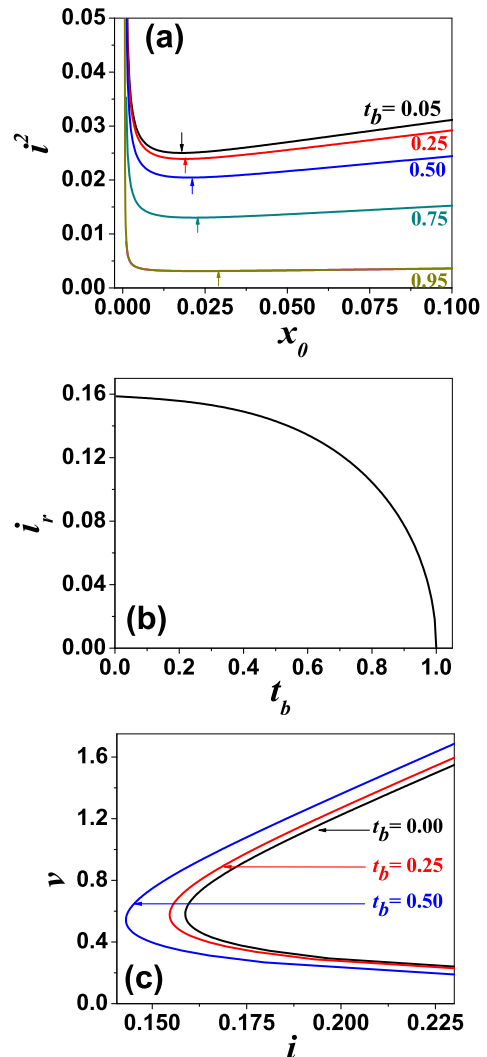


FIG. 3: (a) Plot of Eq. 14 right-hand side as a function of x_0 at different bath temperatures. The minima shown by arrows define the retrapping current i_r . (b) Variation of the retrapping current as a function of the bath temperature. (c) I-V characteristics near i_r at three different bath temperatures as indicated in the figure. The current and the voltage axes are normalized with respect to I_0 and $I_0 R_c$, respectively. All the curves are plotted for $\beta = 3.5$ and $x_1 = 0.015$.

current becomes larger than i_r , does a N-S interface with $T = T_c$ appear at $r_0 (> r_1)$. We will discuss this point in more detail later.

Eq. 14 provides the relation between the current bias I and the N-S interface position x_0 . One can then calculate the resistance $R(x_0)$ using Eq. 2. The related current-voltage characteristic $V = IR(x_0)$ is plotted in Fig. 3c for different bath temperatures. At low voltage, a negative differential resistance branch appears, meaning that, in this regime, for a given current, the voltage can have two distinct values. Since this branch is unstable under current biasing [18], only the higher voltage is accessible. But if one performs voltage-biased measurements, then

one can access the negative differential resistance branch as well, as was observed by Skocpol et al. [11] in microbridges and Steinbach et al. [19] in Josephson junction.

For illustration, let us now consider a WL biased at its retrapping current. Fig. 4 shows the radial temperature distribution for different bath temperatures and for some typical values of β and x_1 . Expectedly, at large distance, the temperature asymptotically decreases to the bath temperature. The temperature profile close to the WL exhibits a large temperature gradient as compared to the superconducting region, see Fig. 4c, d. The intercepts of the different curves with the dotted horizontal lines representing $t = 1$ indicate the location of the N-S interfaces. The temperature values at $x = x_1$ ($= 0.015$ here) indicate the WL temperature.

Still at retrapping, Fig. 5a,b shows the variation of the N-S interface position r_0 in units of r_1 as a function of the bath temperature for different x_1 and β values and as a function of β at a fixed bath temperature for different x_1 values. For large values of β , i.e. for long WLs, the N-S interface is closer to the WL. Fig. 5c and d show the temperature of the WL as a function of the bath temperature for a combination of β and x_1 values. We observe a non-monotonic behavior, which is due to the increase of the thermal conductivity with increasing temperature. The contrast between, on one hand, the monotonic evolution of the current i_r and the N-S interface position x_0 with t_b and, on the other hand, the non-monotonic evolution of the WL temperature at retrapping indicates that it is the size of the normal region and not its local temperature that governs the amplitude of the retrapping current.

III. TRANSPORT EXPERIMENTS ON WEAK LINK μ -SQUIDS

We have tested the above model on μ -SQUID samples. A micrograph of one such device is shown in Fig. 6 inset. We use Nb films deposited using DC magnetron sputtering in a chamber with a base pressure in the 10^{-7} mbar range. For most of the samples, Nb thin films are deposited on a Si wafer and a photo resist is spun on the films. Using optical lithography, we form a coarse pattern (several μm size) on this resist, which is transferred to the film by wet chemical etching using dilute hydrofluoric acid (HF). The final desired pattern is obtained by finer milling with the help of Focused Ion Beam (FIB).

The film thickness d was measured using a profilometer across a step made by masking during deposition. The width w and length ℓ of the WLs were estimated from the SEM images. The sample thickness varies between 30 to 75 nm, whereas the width and length of the WLs vary from 50 to 200 nm. All the WL dimensions are thus much smaller than the length η defined earlier. For most of our devices, the maximum asymmetry between the two junction is less than 10% both in length and width.

In this article, we report on four samples whose detailed parameters are given in Table I. Transport exper-

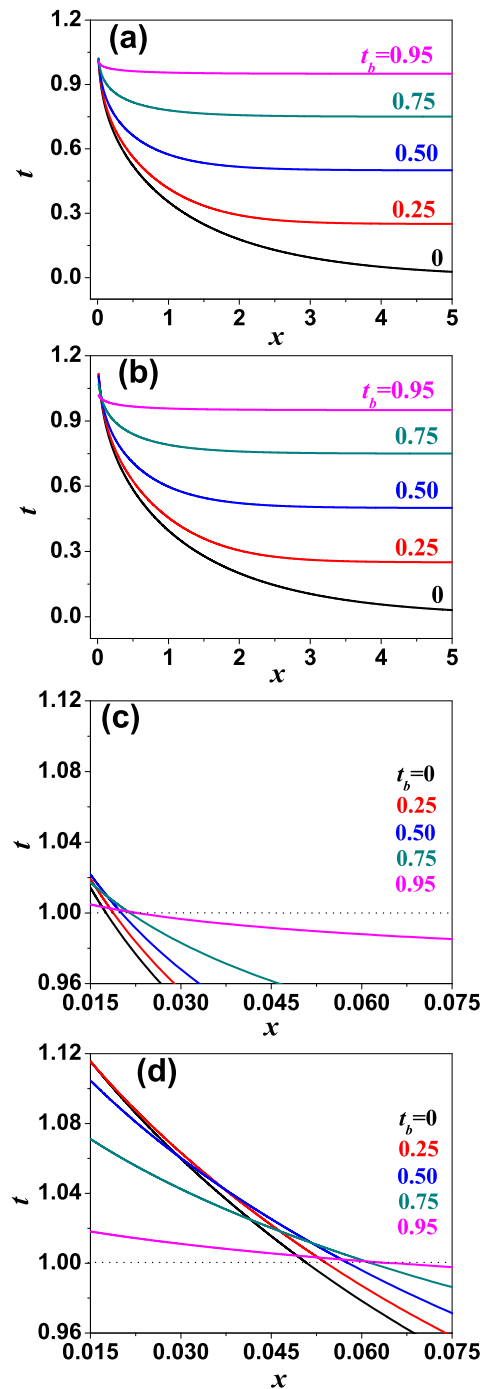


FIG. 4: Temperature (normalized) evolution with radial distance (normalized) in a WL biased at its retrapping current at different bath temperatures indicated in the figures. The parameters are $x_1 = 0.015$ and (a) $\beta = 3.5$, (b) $\beta = 1.5$. (c) and (d) are magnifications near the normal region, corresponding to (a) and (b) respectively. The intersection with the dotted lines at $t = 1$ indicate the N-S interface position.

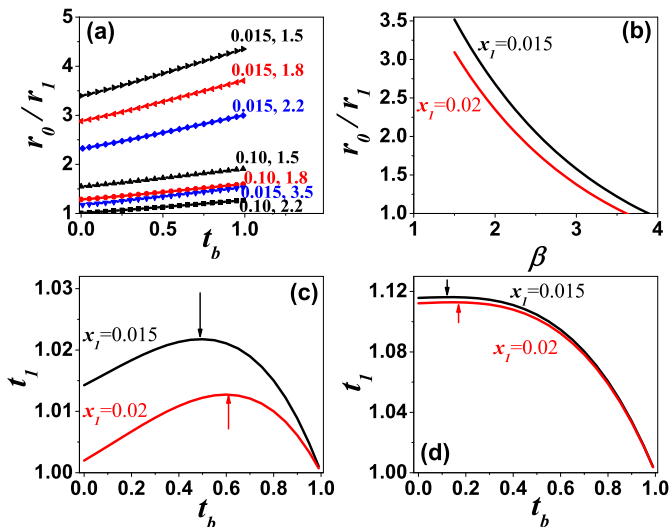


FIG. 5: Variation of the N-S interface position r_0 in units of r_1 at the retrapping current as a function of: (a) bath temperature t_b for different values of x_1 and β , (b) parameter β , at $t_b = 0.15$ for different values of x_1 . (c) and (d) show the variation of the WL temperature at retrapping as a function of bath temperature for (c) $\beta = 3.5$ and (d) $\beta = 1.5$ for $x_1 = 0.015$ and 0.02 . The arrows show the maxima.

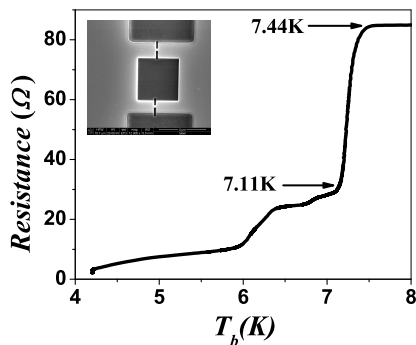


FIG. 6: Resistance vs temperature curve for Sample 2 down to 4.2 K at a bias current of 0.1 mA. Inset shows the SEM image of a typical μ -SQUID with a loop area $3.5 \times 3.5 \mu\text{m}^2$.

iments were performed down to 300 mK in a ^3He cryostat. We used r.f. filters at several stages of the cryostat to minimize noise. Measurements were done in current bias mode using a d.c. current source. No magnetic field was applied for the data presented here.

Fig. 6 shows the temperature variation of Sample 2 resistance down to 4.2 K. The main and sharp transition with an onset at 7.44 K is expectedly for the bulk film. The other transitions (steps) correspond to relatively smaller pads connected to the WLs. Since the resistance has a large tail, it is difficult to define the critical temperature T_c from this data. We therefore define T_c from I-V measurements (discussed below) as the temperature above which I_c is zero, i.e. the I-V curve is ohmic.

Sample 1 I-V characteristics at different bath temper-

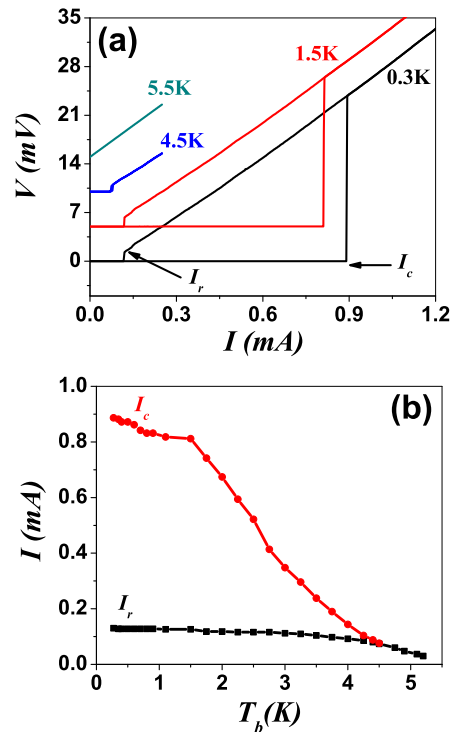


FIG. 7: (a) I-V curve of Sample 1 at four different bath temperatures. The plots of 1.5 K, 4.5 K and 5.5 K have been shifted upwards by 5, 10 and 15 mV, respectively, for clarity. (b) Temperature dependence of the critical and retrapping currents for the same sample.

atures are shown in Fig. 7a. At low temperature, the curves are clearly hysteretic. From this type of data, we experimentally define the critical current as the maximum current up to which no measurable voltage is observed when the current is ramped from zero. Here, we do not distinguish between critical current and switching current. In the retrapping branch, we define the retrapping current as the current at which the resistance goes back to zero. For most of the samples, with the above definitions, the detection of I_c and I_r are accurate within about 1% for $T_b < 1$ K and about 10% near $T_c/2$. Close to T_c , because the transition region width, I_c or I_r cannot be defined with an accuracy better than 50%. Fig. 7b shows the variation of critical I_c and retrapping I_r currents as a function of bath temperature for the same sample. Above a temperature T_h , the retrapping and the critical currents are equal, meaning that hysteresis in the I-V curve has disappeared.

Fig. 8a and b show the experimental $I - V$ at the lowest temperature for the two samples together with their fit by our model. The current and voltage are normalized with respect to the fit-derived parameters I_0 and $R_c I_0$. In Fig. 8c and d, the variation of retrapping current as a function of temperature are shown. Here also the current is normalized with respect to I_0 , whereas the temperature is normalized with respect to the critical

TABLE I: Comparison between various experimental (exp) and fit parameters: WL length ℓ and width w , film thickness d , characteristic resistance R_c , critical temperature T_c , current scale I_0 .

Sam. no.	ℓ (nm)	w (nm)	d (nm)	R_c (exp) (Ω)	R_c (fit) (Ω)	T_c (exp) (K)	T_c (fit) (K)	I_0 (exp) (mA)	I_0 (fit) (mA)
1	95	75	45	2.7 ± 0.3	2.5 ± 0.5	5.50 ± 0.10	5.25 ± 0.53	0.64 ± 0.10	0.81 ± 0.10
2	100	100	55	2.3 ± 0.2	1.6 ± 0.3	5.70 ± 0.10	5.60 ± 0.56	0.77 ± 0.12	0.78 ± 0.09
3	150	145	65	2.0 ± 0.2	1.9 ± 0.3	5.80 ± 0.10	5.60 ± 0.56	0.91 ± 0.14	0.97 ± 0.12
4	150	150	30	5.3 ± 0.5	5.1 ± 0.5	4.5 ± 0.10	4.35 ± 0.44	0.27 ± 0.04	0.24 ± 0.03

temperature T_c . The values of the fit parameters R_c , I_0 and T_c together with the experimental parameters are listed in Table I. Here the experimental $R_c = 2\rho_n/\pi d$ is calculated by measuring the resistance of a known rectangular geometry and $I_0 = 2T_c\sqrt{L_0}/R_c$ is calculated by using the value of above R_c and experimental T_c . We have obtained a similar agreement with Sample 3 and 4 (not shown here), whose experimental and fit parameters are also included in Table I. We have also used the same model for single WLs and μ -SQUIDS from Hasselbach et al. [5] with a different geometry. In both cases, we could fit both the low temperature hysteretic I-V curves and temperature dependence of the retrapping current with our model very well.

Fig. 8d also shows a fit of the retrapping current with the $\sqrt{1-t}$ dependence from Skocpol et al. [11]. The fitted coefficient 0.18 compares reasonably with the estimated value of 0.34, assuming a Wiedemann-Franz law to get the normal-state thermal conductivity. Nevertheless, our model gives a clearly much better agreement, which we attribute to incorporation of the superconductor thermal conductance temperature dependence in our model.

IV. DISCUSSION

The exact thermal model for our system is quite involved with complicated non-linear differential equations. In this paper, we have tried to simplify them in a way that the essential features are preserved. This simplified model fits the experimental data very well. Nevertheless, several approximations need further discussion.

We assumed the width of the connecting pads to be much greater than η , but in actual experiments it is comparable to it. Therefore the actual thermalization would be poorer than what is being assumed; we may be slightly overestimating x_1 . As it is difficult to estimate α for our samples and it actually has a temperature dependence [15], the determination of η and hence x_1 can again be significantly erroneous. For most of the cases, we could fit our data with a 20% variation in the value of x_1 by adjusting the other parameters.

We have made the hypothesis that the electron and phonon temperatures are equal in the superconducting region. The electron-phonon coupling power in a volume V is given by [20], $P = \Sigma V(T_e^5 - T_p^5)$, where $\Sigma =$

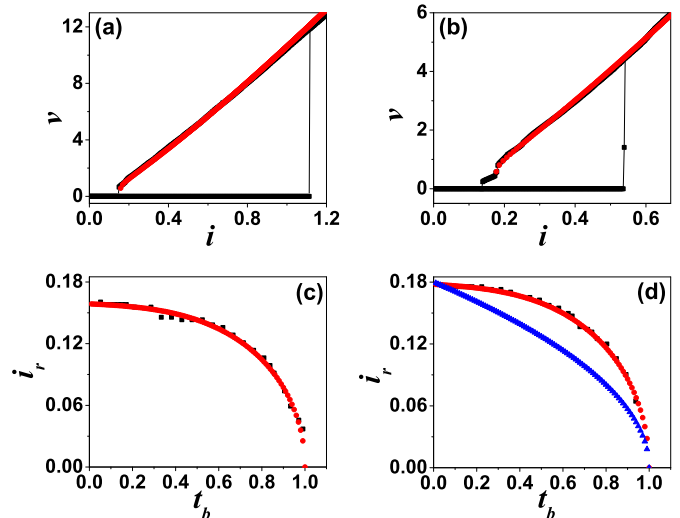


FIG. 8: Experimental (black) and numerical fit (red) of normalized I-V curves for Samples 1 and 2 at $T_b = 300$ mK with (a) $\beta = 3.5$ and $x_1 = 0.015$ for Sample 1 (b) $\beta = 3$ and $x_1 = 0.02$ for Sample 2. (c) and (d): Variation of the normalized retrapping current with the normalized bath temperature for Sample 1 and 2. The black dots are the data and the red curves are fits based on Eq. 14. The fit parameters are listed in Table I. The blue curve in (d) is fitting with the Skocpol et al. [11] (their Eq. 14) prediction $i_r = 0.18(1 - t)^{1/2}$.

$2.4 \times 10^9 \text{ W}\cdot\text{m}^{-3}\text{K}^{-5}$ is the electron-phonon coupling parameter for Nb. Taking typical experimental values $I_r = 0.12$ mA, $R_c = 2.4 \Omega$, $r_0/r_1 = 1.1$ (that gives $R(r_0) = 8 \Omega$), we get a dissipated power $P = I_r^2 R(r_0) = 0.12 \mu\text{W}$. Nearly all of this resistive heat is transmitted to the substrate in the superconducting region only. Though the temperature decreases sharply making the heat loss rather non-uniform, the effective size of this region is of order η , which ranges between 1 and 3 μm . Taking $\eta = 2 \mu\text{m}$, $d = 50$ nm and an average electron temperature $T_e = 4\text{K}$, the volume of the superconducting region is, $V = \pi\eta^2 d = 3.5 \times 10^{-19} \text{m}^3$. This gives the temperature difference $T_e - T_p$ as 0.06 K only, validates our hypothesis.

We took a linear approximation for the surface loss term. The metal film and the substrate phonons exchange heat through a Kapitza resistance, giving a power $K_a(T^4 - T_b^4)$ per surface unit, with K_a as the Kapitza constant [20]. For T close to T_b , the above expression

can be approximated as $4K_a T_b^3 (T - T_b)$. From the temperature profile in Fig.4, we can say that for most of superconducting region the above approximation is valid except for the region close to the N-S interface ($r \simeq r_0$). However, if the bath temperature is close to the critical temperature then for the entire WL the above approximation would be valid.

We also neglected the heat loss to the substrate from the normal region, i.e. the WL and the semicircular region between r_1 and r_0 . Let us compare the heat transfer to the substrate P_s and the heat conducted out P_c under the linear approximation. Considering only one half of the film, we can approximately write $P_s = \alpha \pi r_0^2 (t_1 - t_b) T_c / 2$. We can also write $P_c = -\kappa_n \pi r_0 d \left(\frac{dT}{dr} \right)_{r=r_0} = \pi r_0 d L_0 T_c^2 (t_1 - 1) / (\rho_n (r_0 - r_1))$. Here we assume a linear temperature decrease within the normal region, which is fairly justified according to Fig. 4c, d. For $t_1 = 1.1$, $t_b = 0.05$, $r_1 = 100$ nm, $r_0 = 2r_1$, $\alpha = 5$ W/cm².K, $d = 50$ nm, $\rho_n = 25$ $\mu\Omega$ cm, and $T_c = 8$ K, one gets $P_c = 0.2$ μ W and $P_s/P_c \simeq 0.1$, which confirms our assumption.

The surface heat loss from the WL normal state region was neglected by assuming $(t_1 - t_b) \frac{A}{2\pi\eta^2} \ll \beta i^2$. Let us check the argument for the worst possible case; i.e. at lowest possible temperature and for longer WLs. Taking $t_b = 0.05$, $t_1 = 1.1$, $A = 300 \times 300$ nm², $\eta = 1$ μ m at $i = i_r = 0.15$, one gets $(t_1 - t_b) \frac{A}{2\pi\eta^2} = 0.015$, whereas with $\beta = \pi$ (which corresponds to $\ell = w = 300$ nm) and $i = i_r = 0.15$ we get $\beta i^2 = 0.072$, which is almost 5 times higher than $(t_1 - t_b) \frac{A}{2\pi\eta^2}$.

V. WHEN DOES HYSTERESIS DISAPPEAR?

A key feature is the disappearance of hysteresis at high temperature. In general, there is a particular bath temperature T_h at which I_r and I_c are equal. Above this temperature, for $I > I_c$ the current is large enough to kill the superconductivity in the WL, making it resistive. But the related Joule heating is not sufficient to raise the WL temperature above T_c and provide an N-S interface. In order to find the crossover temperature T_h , we need an expression for the temperature dependence of the critical current. For a bath temperature near the critical temperature, we can use the expression: [1, 21] $I_c R_n = \gamma T_c (1 - t_b)$, where $\gamma = 635$ μ V/K and R_n is the normal state resistance. In practice, γ can vary significantly. Taking $R_n = R_0$, one can simplify the above equation to:

$$i_c = \frac{\gamma}{2\beta\sqrt{L_0}} (1 - t_b). \quad (15)$$

Here, $i_c = I_c/I_0$ and we have used $\gamma = 635$ μ V/K, $L_0 = 2.44 \times 10^{-8}$ W. Ω /K². In Fig. 9, we plot the variation of I_c with the bath temperature for Sample 1 above $T_c/2$. From the linear fit, we extract $\gamma = 930$ μ V/K with the above L_0 value, $\beta = 3.5$ and $R_c = 2.28\Omega$.

In Fig. 10, we plot the variation of i_c (red curve) and i_r (black curve) as a function of the normalized bath

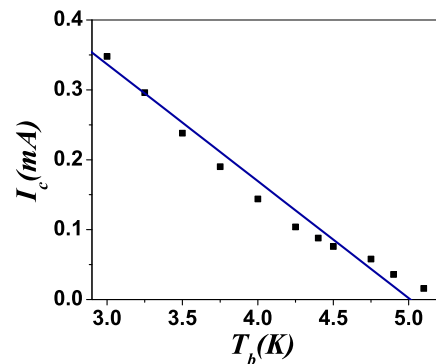


FIG. 9: Variation of critical current with the bath temperature in the high temperature regime for Sample 1. The blue line is a straight line fitting $I_c = I_{c0}(1 - T_b/T_c)$ with $I_{c0} = 0.84$ mA and $T_c = 5.05$ K.

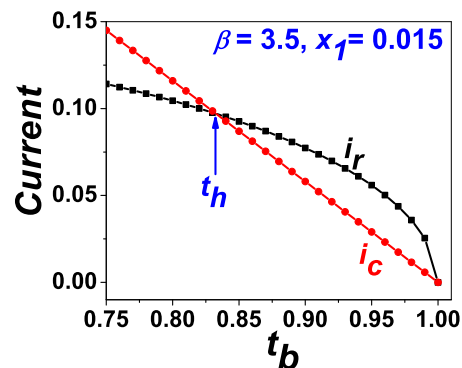


FIG. 10: Temperature dependence of i_c (red) following Eq. 15 and of i_r (black) calculated from our model, near the critical temperature. The parameters used for the plot are given in the figure. At $t_b = t_h$, the two curves cross each other, so that hysteresis disappears for higher temperatures.

temperature t_b near $t_b = 1$ using Eq. 15, for $\beta = 3.5$ and $x_1 = 0.015$. The crossover temperature t_h is then straightforwardly determined from the intercept of the two curves. Let us point out here that the critical current I_c and the retrapping current I_r are controlled by two different physics, with I_c dependent on the WL superconducting properties and I_r on the heat dissipation. This justifies that these currents have a different temperature dependence.

In Fig. 11, we plot the variation of t_h as a function of β for three different values of x_1 . The top axis refers to ℓ/w , which is related to β by the formula: $\beta = \frac{\pi}{2}(1 + \frac{\ell}{w})$. The upper limits β_{max} of the parameter β are chosen in a way that at this point $x_0 = x_1$, i.e. the N-S interface is at the WL boundary, as beyond this value our short WL approximation does not hold. From Fig. 11, this occurs at a t_h of about 0.8.

In the hysteresis-free regime $t > t_h$, the detailed temperature profile $i_r > i > i_c$ can be found by solving Eq. 10 for $x > x_1$, i.e. the superconducting region. The boundary conditions used for solving this equation are 1)

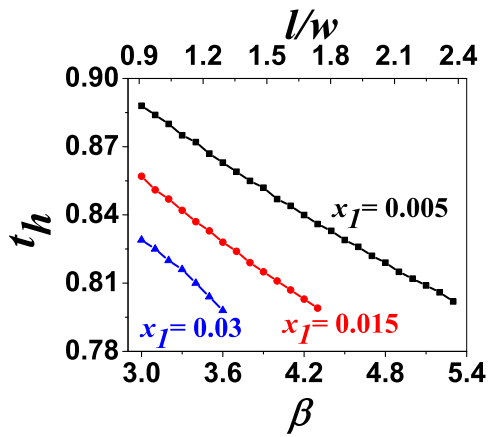


FIG. 11: Variation of the hysteresis crossover temperature t_h with the parameter β for three different values of x_1 (i.e. WL width). The top axis represents ℓ/w , calculated using the formula: $\beta = \frac{\pi}{2}(1 + \frac{\ell}{w})$.

at $x = x_1$, $-x_1 t_1 \frac{dt}{dx} = \frac{\pi d R_0 i^2}{2 \rho_N}$ and 2) $t = t_b$ as $x \rightarrow \infty$. Solutions for t were found numerically and are plotted in Fig. 12a.

Fig. 12b shows the temperature t_1 of the WL as a function of current for two bath temperatures, $t_b = 0.90$ and $t_b = 0.75$, respectively above and below the hysteresis threshold $t_h = 0.83$. As the current is ramped up from zero, the WL temperature jumps from $t_1 = t_b$ to a higher value at $i = i_c$. For a bath temperature above the hysteresis threshold ($t_b > t_h$), there is another jump in WL temperature at $i = i_r$ and after this the temperature keeps on increasing. The t_1 vs i behavior remains same when i is ramped down, i.e. there is no hysteresis. Let us point out that there is no actual retrapping at this i_r value, but the appearance or disappearance of a N-S interface close to the WL. For a bath temperature below the hysteresis threshold ($t_b < t_h$), the behavior shows an upward jump from $t_1 = t_b$ to a higher value when the current is ramped up through $i = i_c$, and a downward jump to $t_1 = t_b$ when current is ramped down through $i = i_r$. Hysteresis is thus present.

Fig. 12c shows the $i-v$ curves as calculated from the location of the N-S interface (above i_r) and the resistance of the WL (below i_r) at the same two bath temperatures above and below t_h . We see a close resemblance between the temperature and voltage curves as a function of bias current. While below t_h , the $i-v$ spectra describe well the experimental curve, above t_h the calculated curve shows an extra step at i_r arising from the sudden creation of the N-S interface at a position $r_0 > r_1$. This step was not observed in experiments. We believe that the predicted extra step may get significantly rounded as the WL temperature approaches T_c . The superconducting region outside r_1 will be close to T_c , reducing its critical current density. The exact shape of the I-V curve in the non-hysteretic regime will then be dictated by thermally activated phase slips [22, 23] for $i < i_c$ and

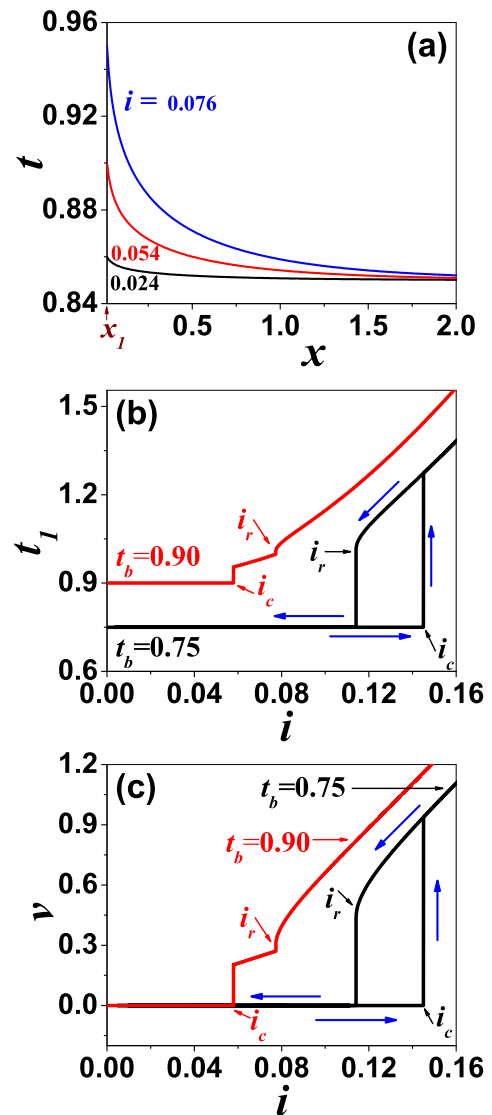


FIG. 12: Calculation results with parameters β and x_1 equal to 3.5 and 0.015 respectively, which give $t_h = 0.83$. (a) Calculated temperature distribution at a bath temperature $t_b = 0.85$ above the threshold temperature t_h for normalized bias currents of 0.024, 0.054 and 0.076. Here i_r is 0.093. (b,c) Variation of WL temperature (b) and $i-v$ curve (c) as a function of bias current for bath temperatures above the threshold $t_b = 0.75$ (black) and below $t_b = 0.90$ (red). The blue arrows indicate the direction of current sweep.

superconducting fluctuations for $i > i_c$ [23].

Let us now consider how one could manipulate the crossover temperature t_h . At a fixed x_1 (which is proportional to the width w), t_h decreases with the increase of β (and hence the length ℓ), see Fig. 11. This is desirable if we want hysteresis to disappear at low temperature. But the adjustment of β to any arbitrary value is impossible, since we wish the WL to behave like a Josephson Junction, which implies the condition: $w \leq \ell \sim \xi$ [1]. This gives a lower bound on β and x_1 and hence t_h in general.

Therefore, it is generally not possible to eliminate hysteresis for these WL junctions just by manipulating the WL width and length.

However, since β is the ratio of WL resistance R_0 to the characteristic resistance R_c of the film, we can effectively increase β by increasing the WL resistance. This can be done by reducing the thickness of the WL alone. The reduction of the whole film thickness (d) including the connecting electrodes can also reduce T_h : in this case, $\eta \propto \sqrt{d}$ is smaller, giving a larger x_0 . This makes hysteresis disappear at smaller temperatures (see Fig. 11). If the critical temperature T_c is not affected, a wider temperature span for the hysteresis-free regime is achieved. This improvement was observed by Tinkham et al. [14] for superconducting nano-wires. With an appropriate choice of substrate and growth conditions, the resistivity and critical temperature of very thin films can remain almost unaffected by thickness reduction (for Nb see Ref. 24), enabling similar results to be obtained with continuous films. Another possible way is to reduce the critical current I_c (and possibly increase β) by either making the WL with a poor superconductor or completely replacing it by a normal metal. Angers et al. [7] were able to get a $T_h < 1.2K$ for μ -SQUIDS made with SNS type weak links based on Nb.

VI. CONCLUSIONS

In conclusion, we have described a thermal model for understanding the hysteresis in the I-V curve of short

superconducting WLs and their extension to μ -SQUIDS. Using this model, we have calculated the detailed I-V characteristics and the temperature profile near the WL as a function of bath temperature. We have obtained a good agreement between experiments and theory in terms of I-V characteristics and their temperature dependence. A key finding of this model, which again is in agreement with the experiments, is the disappearance of hysteresis above certain temperature. We have discussed how one can adjust the WL geometry in order to widen the temperature range of this hysteresis-free regime of WL-based μ -SQUIDS.

VII. ACKNOWLEDGEMENTS

DH acknowledges the financial support from CSIR, India and the French Embassy in India. Discussions with Klaus Hasselbach have been fruitful. Sincere thanks to Sudhanshu Srivastava for help with FIB, Prabhat Kumar Dwivedi for his help in optical lithography. Thanks to Franck Dahlem, Thomas Quaglio and Soumen Mandal for helping in some of the technical matters. LP acknowledges financial support from Région Rhône-Alpes. AKG thanks Université Joseph Fourier, Grenoble for its support during his visit in 2009.

-
- [1] K. K. Likharev, Rev. Mod. Phys. **51**, 101 (1979).
 - [2] M. Tinkham, Introduction to Superconductivity 2nd ed. (Mc Graw-Hill, New York, 1996).
 - [3] W. Wernsdorfer, Adv. Chem. Phys. **118**, 99 (2001).
 - [4] W. Rabaud, L. Saminadayar, D. Mailly, K. Hasselbach, A. Benoit, and B. Etienne, Phys. Rev. Lett. **86**, 3124 (2001).
 - [5] K. Hasselbach, C. Veauvy, D. Mailly, Physica C **332**, 140 (2000).
 - [6] S. A. Makhlof, F. T. Parker, F. E. Spada, and A. E. Berkowitz, J. Appl. Phys. **81**, 5561 (1997); S. D. Tiwari and K. P. Rajeev, Phys. Rev. B **72**, 104433 (2005).
 - [7] L. Angers, F. Chiodi, G. Montambaux, M. Ferrier, S. Guéron, H. Bouchiat, and J. C. Cuevas, Phys. Rev. B **77**, 165408 (2008).
 - [8] M. S. Crosser, Jian Huang, F. Pierre, P. Virtanen, T. T. Heikkilä, F. K. Wilhelm, and N. O. Birge, Phys. Rev. B **77**, 014528 (2008).
 - [9] A. Rogachev, A. T. Bollinger, and A. Bezryadin, Phys. Rev. Lett. **94**, 017004 (2005).
 - [10] T. A. Fulton and L. N. Dunkleberger, J. Appl. Phys. **45**, 2283 (1974).
 - [11] W. J. Skocpol, M. R. Beasley, and M. Tinkham, J. Appl. Phys. **45**, 4054 (1974).
 - [12] Y. Song, J. Appl. Phys. **47**, 2651 (1976).
 - [13] H. Courtois, M. Meschke, J. T. Peltonen, and J. P. Pekola, Phys. Rev. Lett. **101**, 067002 (2008).
 - [14] M. Tinkham, J. U. Free, C. N. Lau, and N. Markovic, Phys. Rev. B **68**, 134515 (2003).
 - [15] C. Peroz and C. Villard, Phys. Rev. B **72**, 014515 (2005). Here, instead of α , the authors have used symbol h .
 - [16] E. T. Swartz and R. O. Pohl, Rev. Mod. Phys. **61**, 605 (1989); A.I. Bezuglyj and V.A. Shklovskij, Physica C **202**, 234 (1992).
 - [17] A. A. Abrikosov, Fundamentals of the Theory of Metals (Elsevier Science, Amsterdam, 1988); see also Fig.1 and 2 in F. Koechlin and B. Bonin, Supercond. Sci. Technol. **9**, 453 (1996).
 - [18] B. K. Ridley, Proc. Phys. Soc. **82**, 954 (1963).
 - [19] A. Steinbach, P. Joyez, A. Cottet, D. Estève, M. H. Devoret, M. E. Huber, and John M. Martinis, Phys. Rev. Lett. **87**, 137003 (2001).
 - [20] F. C. Wellstood, C. Urbina, and J. Clarke, Phys. Rev. B **49**, 5942 (1994).
 - [21] Here, instead of γ , Likharev [1] used the symbol α . Since we have already used α for surface heat loss coefficient, here we use a different symbol.
 - [22] A. Bezryadin, J. Phys. Condens. Mat. **20**, 043202 (2008).
 - [23] W. J. Skocpol and M. Tinkham, Rep. Prog. Phys. **38**, 1049 (1975).

- [24] V. Bouchiat, M. Faucher, C. Thirion, W. Wernsdorfer, T. Fournier, and B. Pannetier, *Appl. Phys. Lett.* **79**, 123 (2001).

